

Oligomerization-Dependent Folding of the Membrane Fusion Protein of Semliki Forest Virus

HELENA ANDERSSON,[†] BERND-UWE BARTH,[‡] MARIA EKSTRÖM, AND HENRIK GAROFF*

Department of Biosciences at Novum, S-141 57 Huddinge, Sweden

Received 30 May 1997/Accepted 2 August 1997

The spikes of alphaviruses are composed of three copies of an E2-E1 heterodimer. The E1 protein possesses membrane fusion activity, and the E2 protein, or its precursor form, p62 (sometimes called PE2), controls this function. Both proteins are, together with the viral capsid protein, translated from a common C-p62-E1 coding unit. In an earlier study, we showed that the p62 protein of Semliki Forest virus (SFV) dimerizes rapidly and efficiently in the endoplasmic reticulum (ER) with the E1 protein originating from the same translation product (so-called heterodimerization in *cis*) (B.-U. Barth, J. M. Wahlberg, and H. Garoff, *J. Cell Biol.* 128:283–291, 1995). In the present work, we analyzed the ER translocation and folding efficiencies of the p62 and E1 proteins of SFV expressed from separate coding units versus a common one. We found that the separately expressed p62 protein translocated and folded almost as efficiently as when it was expressed from a common coding unit, whereas the independently expressed E1 protein was inefficient in both processes. In particular, we found that the majority of the translocated E1 chains were engaged in disulfide-linked aggregates. This result suggests that the E1 protein needs to form a complex with p62 to avoid aggregation. Further analyses of the E1 aggregation showed that it occurred very rapidly after E1 synthesis and could not be avoided significantly by the coexpression of an excess of p62 from a separate coding unit. These latter results suggest that the p62-E1 heterodimerization has to occur very soon after E1 synthesis and that this is possible only in a *cis*-directed reaction which follows the synthesis of p62 and E1 from a common coding unit. We propose that the p62 protein, whose synthesis precedes that of the E1 protein, remains in the translocon of the ER and awaits the completion of E1. This strategy enables the p62 protein to complex with the E1 protein immediately after the latter has been made and thereby to control (suppress) its fusion activity.

Enveloped viruses penetrate into the cytoplasm of cells by fusing their own membrane with that of their host (73). For this purpose, these viruses carry spike proteins with membrane fusion activity. To ensure that fusion occurs only at the correct cell membrane, the fusion function of the spike has to be tightly controlled. This requirement implies that the fusion protein, or fusogen, has to be synthesized in an inactive form, which can be converted into an active form at the correct moment. The mechanism for controlling membrane fusion is today best known for influenza virus. The fusogen of this virus is a homotrimeric spike protein, the hemagglutinin (HA), which also contains the binding site for the host receptor (74). After synthesis in the endoplasmic reticulum (ER), the HA monomers are fusion inactive (11, 61, 67). They enter a common pool in the ER from which trimers are generated randomly (10). The trimers are then transported to the plasma membrane, where they take part in virus formation (53). When passing through the trans-Golgi apparatus, HA is cleaved into an external HA₁ part and a transmembrane HA₂ part by a furinlike enzyme (64). This cleavage provides the first step in the process of activation of the fusogen (38, 74). The second step is provided by the low pH that the virus encounters when it enters the endosome of the host cell (45, 74). Structural analyses have revealed that HA₁ dissociates from HA₂ and that large conformational changes take place in HA₂ at this step (14, 22, 57, 75). In particular, there is a transition of the hairpin

structures that the three HA₂ chains form at their NH₂-terminal regions into a helical coiled-coil. Through this alteration, the so-called fusion peptide, which is located at the NH₂-terminus of HA₂, is displaced from a protected internal location to the very tip of the spike. This conformational change most likely elicits the fusion activity. Structural studies with peptides comprising the loop region of the HA₂ hairpin have suggested a spring-loaded mechanism to explain the conformational change (17). Accordingly, the hairpin represents a kinetically trapped, metastable conformation that is generated during the initial folding of HA. In the cleaved HA molecule, this conformation is maintained through HA₁-HA₂ interactions. However, when HA₁ is dissociated from HA₂ by the low endosomal pH, the energy barrier imposed by these interactions is removed, and the hairpin adopts its stable coiled-coil conformation.

It is reasonable to assume that similar mechanisms are used by other enveloped viruses, especially those which carry influenza virus-like cleavable homo-oligomeric spike proteins (e.g., retrovirus) (5, 23, 24, 35, 42). However, in many viruses, e.g., alphaviruses, flaviviruses, rubellavirus, pestiviruses, and hepatitis C virus, the spikes are composed of heterodimeric protein complexes in which the fusion protein itself remains uncleaved (3, 54, 55, 58, 72, 77). In these cases, it is the association of the fusion protein with the other protein that controls the fusion activity (2, 12, 33, 36, 69). We have been interested in the mechanism of fusion activation in such spikes. For this purpose, we are studying the alphavirus Semliki Forest virus (SFV).

The spike protein monomers of SFV, i.e., p62 (62 kDa) and E1 (50 kDa), are synthesized together with the capsid (C) protein (33 kDa) and the 6K peptide (6 kDa) by use of a common C-p62-6K-E1 coding unit on the subgenomic 26S

* Corresponding author. Mailing address: Department of Biosciences at Novum, S-141 57 Huddinge, Sweden.

[†] Present address: Department of Pharmacology, Basel University, Biozentrum, CH-4056 Basel, Switzerland.

[‡] Present address: Département de Biologie Cellulaire, Université de Genève, CH-1211 Geneva, Switzerland.

RNA (28). The C protein is released from the growing polypeptide chain through its autoproteolytic activity, and the membrane proteins, including the small 6K peptide, are separated from each other by the host signal peptidase (1, 4, 6, 8, 19, 27, 29, 31, 32, 39, 46, 47). The p62 and E1 proteins oligomerize in the ER into p62-E1 heterodimers (4, 50, 78). These are transported to the cell surface, where they interact with the nucleocapsid (NC) protein and thereby drive virus budding (13, 66). During transport through the trans-Golgi apparatus, the p62 protein is cleaved into a small external part (E3) and a larger, membrane-bound part (E2) (20). At some stage during the assembly process, possibly in the ER, the heterodimers trimerize and form viral spikes (18, 48, 52, 68). SFV enters its host cells via the endocytotic pathway (44), and the membrane fusion is most likely mediated by the E1 protein (26, 37, 51, 56). In the infected cell, this function is suppressed through association of the E1 protein with the p62 protein (41, 59). Cleavage of p62 into E2 and E3 represents the first activation step, rendering the complex sensitive to low-pH-induced dissociation (70). Thus, when the virus enters the endosome, the low pH can act as a second and final triggering event. It allows the E1 protein to release itself from E2 and to oligomerize into a stable homotrimer (12, 25, 36, 69, 71). This process elicits the membrane fusion activity.

An interesting question is how the E1 fusogen is synthesized. In analogy with the HA₂ part of influenza virus HA, this protein also probably has to be trapped in a metastable conformation with a suppressed fusion function. However, in contrast to HA, E1 itself does not necessarily have the capacity to suppress its fusion activity; this is a function of the p62 protein with which the E1 protein forms a complex. Therefore, it appears less likely that newly synthesized E1 molecules form a common pool of oligomerization-competent monomers in the ER like HA does. Instead, immediate capture of newly synthesized metastable E1 by p62 is expected. In order to ensure rapid oligomerization, the sequential synthesis of p62 and E1 from a common mRNA seems to be a reliable solution. Indeed, we recently showed that the p62-E1 heterodimerization reaction involves preferentially p62 and E1 monomers that have been generated from the same translation product (so-called heterodimerization in *cis*) (4). In the present work, we have addressed the question of whether correct synthesis of the E1 fusogen requires p62. To find out, we constructed two variants of the SFV cDNA clone (40): one with a p62 gene deletion and another with an E1 gene deletion. The corresponding replication-competent RNAs were transcribed in vitro and used to transfect BHK-21 cells. The synthesis of E1 and p62 was then monitored and compared with that of the two membrane proteins expressed from their common coding unit on the SFV 26S RNA.

MATERIALS AND METHODS

Cells, plasmids, and antibodies. Baby hamster kidney (BHK-21) cells were grown in Glasgow minimal essential medium (Glasgow MEM [BHK-21] with L-glutamine and without tryptose phosphate broth; GIBCO BRL, Paisley, United Kingdom) supplemented with 10% tryptose phosphate broth, 5% fetal calf serum, 20 mM HEPES (pH 7.3), and 2 mM glutamine. Penicillin (100 U/ml) and streptomycin (100 mg/ml) were also added to the medium for cell culturing. For immunoprecipitations, monoclonal antibody UM 8.139 against E1 and a polyclonal rabbit antiserum against E1 were used (7, 70).

Plasmids encoding complete or mutant SFV sequences were as follows: (i) pSFV4, which contains the wild-type genome (39); (ii) pSFV-C-E1, which contains, in the following order, the C gene, the first three codons of the p62 gene, two codons derived from a *Bam*HI site, two codons coding for Arg residues, the last 18 codons of the 6K gene (encoding the E1 signal sequence), and the E1 gene; (iii) pSFV-p62Δa, which lacks the codons for amino acids 4 to 457 of the p62 protein; (iv) pSFV-p62Δb, which lacks the codons for amino acids 67 to 416 of the p62 protein; (v) pSFV-p62Δc, which lacks the codons for amino acids 242 to 416 of the p62 protein; (vi) pSFV-p62Δd, which lacks the codons for amino

acids 67 to 241 of the p62 protein; (vii) pSFV-C-p62, which encodes amino acid sequences for C and p62 (including 6K) (3a); and (viii) pSFV-E1, which contains the E1 gene but not the C and p62 genes (3a). Plasmids pSFV-p62Δa, pSFV-p62Δb, pSFV-p62Δc, and pSFV-p62Δd were made by PCR (34, 76). All fusion sites were confirmed by DNA sequencing. In all of the plasmids, the SFV sequences can be transcribed by SP6 polymerase into RNA molecules which are competent for replication in cells.

Transfection of RNA into cells. RNA was made by transcription of plasmid DNA in a 50-μl mixture as described previously (39). For electroporation, 5 × 10⁶ BHK-21 cells were mixed with 20 μl of transcription mixture. Electroporation was performed at room temperature by two consecutive pulses at 850 V and 25 μF. Efficient transfection was achieved by thoroughly suspending cells beforehand by trypsinization and gentle mixing. After transfection, the cells were diluted 20-fold with BHK medium (GIBCO BRL, Paisley, United Kingdom), distributed into 35-mm dishes, and incubated at 37°C in a 5% CO₂ atmosphere.

Metabolic labelling of viral proteins. Transfected cells were usually labelled (pulsed) at 7 h after electroporation. For 10⁶ cells, we used 50 μCi of [³⁵S]methionine (specific activity, >37 TBq/mmol or >1,000 Ci/mmol; Amersham International plc, Buckinghamshire, England) in 500 μl of labelling medium (MEM without L-methionine; GIBCO BRL). Cells were starved for 30 min before labelling. The pulse was terminated by changing the medium to MEM containing 10×-concentrated unlabelled methionine. The chase in this medium was continued for different times.

Preparation of cell lysates. Immediately after the pulse or at the end of the chase, cells were placed on ice, washed with ice-cold phosphate-buffered saline, incubated for 5 min on ice in phosphate-buffered saline containing 20 mM N-ethylmaleimide, and solubilized in 300 μl of Nonidet P-40 (1%) lysis buffer (70) containing 10 mg of phenylmethylsulfonyl fluoride per ml and 20 mM N-ethylmaleimide. Lysates were cleared by centrifugation at 5,000 × g for 5 min at 4°C.

Processing of lysates. One hundred microliters of cell lysate was used for immunoprecipitation as described before (70). For endoglycosidase H (Endo H; Boehringer GmbH, Mannheim, Germany; 5 mU/μl) treatment of a cell lysate, 5 μl of the latter was mixed with 20 μl of Endo H buffer, which contained 50 mM sodium citrate (pH 6.0) and 1% sodium dodecyl sulfate (SDS). One microliter of Endo H was added, and the mixture was incubated for 16 h at 37°C. Then, two 10-μl aliquots of the reaction mixture were processed for SDS-polyacrylamide gel electrophoresis (PAGE) under reducing and nonreducing conditions. For analyses under reducing conditions, 5 μl of 4×-concentrated SDS gel loading buffer (see below), 4 μl of 20% SDS, and 2 μl of 0.5 M dithiothreitol (DTT) were added. The sample was incubated at 95°C for 2 min before it was loaded on the gel. For analyses under nonreducing conditions, the sample was treated similarly, but DTT was omitted and incubation was done at 70°C. A second lysate sample was processed in the same way but without Endo H.

For Endo H treatment of an immunoprecipitated lysate sample, the precipitate was mixed with 50 μl of Endo H buffer, incubated for 5 min at 70°C, and centrifuged. The supernatant with viral proteins was divided into two parts, which were Endo H treated (2.5 μl of enzyme) and mock treated. Incubation was done for 6 h at 37°C. Then, each sample was again divided in two for SDS-PAGE under reducing and nonreducing conditions.

When lysates were analyzed directly, 10 μl of lysate was mixed with 5 μl of 4×-concentrated gel loading buffer, 4 μl of 20% SDS, and 1 μl of H₂O. Before being loaded on the gel, the mixture was incubated at 70°C for 2 min. For analyses under reducing conditions, 2 μl of 0.5 M DTT was added and incubation was done at 95°C.

SDS-PAGE. All samples were taken up in SDS gel loading buffer, which contained 200 mM Tris-HCl (pH 8.8), 20% glycerol, 5 mM EDTA, 0.02% bromophenol blue, 1 mM methionine, and 4% SDS. The composition of the gel electrophoresis system has been described before (63). After SDS-PAGE, the gel was treated for fluorography with 1 M sodium salicylate for 30 min and then dried. Quantitation of the radioactivity in the viral protein bands was done with a Fuji imaging plate scanner system type FUJIX. The C protein was used as an internal standard when we compared the amounts of viral proteins in reduced and nonreduced lysate samples. Molar ratios were calculated after normalizing the PSL counts of the proteins to their methionine contents.

RESULTS

Synthesis of p62 and E1 in cells transfected with SFV wild-type RNA. Parallel cultures of BHK-21 cells transfected with SFV wild-type RNA were pulse-labelled with [³⁵S]methionine for 2 min and then lysed directly or after a chase for 1, 5, or 15 min. The translocation of p62 and E1 was analyzed by SDS-PAGE with reduced samples that were either incubated with Endo H or mock treated. Immunoprecipitation was unnecessary because of the efficient shutoff of host protein translation in cells transfected with replication-competent SFV RNA. The analyses showed that cleaved and glycosylated E1 and p62 appeared together with C and a 97-kDa protein already in the

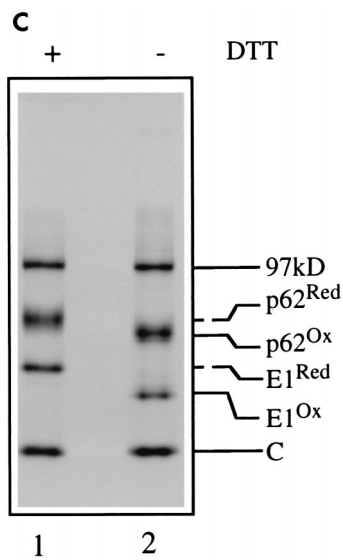
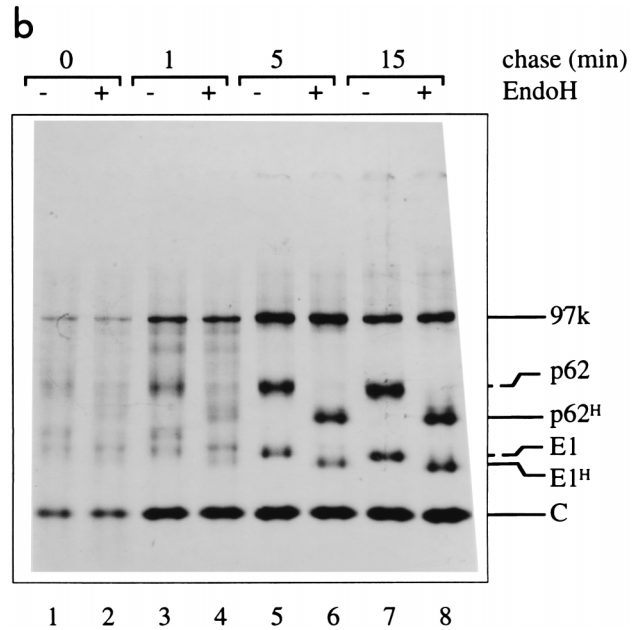
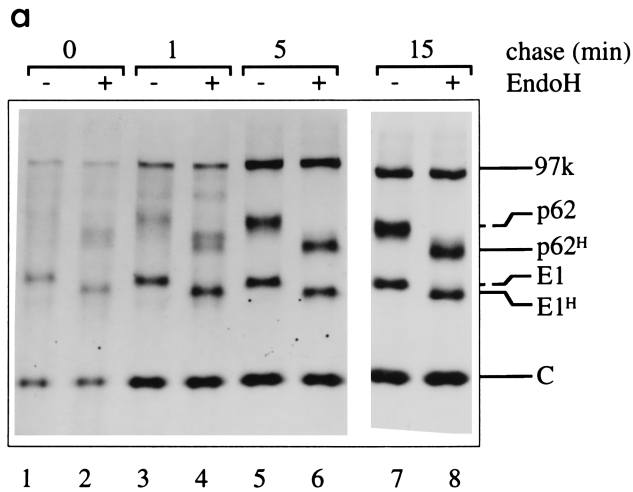


FIG. 1. Translocation and folding of viral membrane proteins in cells transfected with SFV wild-type RNA. Transfected cells were metabolically labelled with [³⁵S]methionine for 2 min and chased for 0, 1, 5, and 15 min. The lysates were either mock treated or Endo H treated and analyzed by SDS-PAGE under reducing (a) or nonreducing (b) conditions. (c) Equal portions of reduced and nonreduced samples from cells chased for 5 min were run next to each other. Superscript H, Endo H-digested protein; superscript Red and Ox, reduced and oxidized forms of a protein, respectively. Note that lanes 1 to 6 and lanes 7 and 8 in panel a were derived from different gels. All panels represent autoradiographs.

unchased samples (Fig. 1a, lanes 1 and 2). The corresponding protein bands became more distinct and stronger in samples chased for 1 and 5 min (Fig. 1a, lanes 3 to 6). This increase in labelling in viral proteins during the chase is expected if one considers the length of the C-p62-6K-E1 coding region in the subgenomic 26S RNA and the time it takes for the chase to become effective after the corresponding medium is added to the cells. The 97-kDa protein has been characterized before (4, 29). It represents untranslocated and hence unglycosylated p62-6K-E1 polyprotein. This form is generated as a result of unsuccessful initiation of chain translocation into the ER during translation of the viral membrane proteins from the 26S RNA. Quantitation of viral proteins in SDS gel analyses of samples chased for 5 min showed that about 30% of the synthesized p62 and E1 chains remained untranslocated as the 97-kDa protein.

An SDS-PAGE analysis under nonreducing conditions allowed us to assess the fractions of E1 and p62 that have established correct intramolecular disulfide bridges during their folding in the ER. Due to a more compact structure, the fully oxidized forms of E1 or p62 move faster in an SDS gel during electrophoresis than both partially folded and fully re-

duced E1 or p62 forms. The analyses showed that a fast-moving E1 band, corresponding to fully oxidized E1, was clearly present in samples from cells chased for 5 min or more (Fig. 1b, lanes 5 and 7). A corresponding band could also be detected in samples from cells chased for 1 min or not chased at all (Fig. 1b, lanes 1 and 3). In addition, these latter analyses demonstrated the presence of a somewhat slower-moving band which contained Endo H-sensitive protein (Fig. 1b, lanes 1 to 4). This might represent an E1 folding intermediate. An apparently fully oxidized p62 was clearly observed in samples from cells chased for 1 min or more (Fig. 1b, lanes 3, 5, and 7). This band was also weakly visible in samples from unchased cells (Fig. 1b, lane 1). However, in contrast to the results for E1, we were not able to identify apparent folding intermediates of p62.

In order to measure the efficiency of p62 and E1 folding into their fully oxidized forms, we analyzed reduced and nonreduced samples in parallel by SDS-PAGE and compared the amounts of labelled p62 and E1 proteins that were found in the corresponding bands. p62 and E1 found in the reduced samples represented the total fractions of translocated and glycosylated chains, whereas the nonreduced samples yield the fractions that are correctly oxidized. Figure 1c shows an analysis of reduced and nonreduced samples of cells chased for 5 min. It is evident that the oxidized forms of p62 and E1 migrated faster than the corresponding reduced ones. Quantitation of the labelled proteins in three separate analyses showed that correctly oxidized p62 and E1 represented about 90 and 80%, respectively, of the total translocated membrane protein chains. We conclude that the large majority of the translocated chains become correctly oxidized and hence probably also cor-

rectly folded. An earlier study showed that these folded p62 and E1 proteins very efficiently form heterodimers in *cis* (that is, complexes involving membrane proteins that originate from the same round of 26S RNA translation) (4).

Translocation and folding of E1 in cells transfected with SFV C-E1 RNA. E1 synthesis in SFV C-E1 RNA-transfected cells was analyzed in the same way as in SFV wild-type RNA-transfected cells. SDS-PAGE analyses of reduced samples showed the presence of a band which migrated like control E1 (Fig. 2a, lanes 2, 4, 6, and 8). After Endo H treatment, an additional band with a higher mobility appeared (Fig. 2a, lanes 3, 5, 7, and 9). This result suggests that both Endo H-resistant and -sensitive forms of E1 are produced in transfected cells. The former most likely represents untranslocated and hence unglycosylated E1 chains, whereas the latter corresponds to translocated and glycosylated E1. The lower mobility of untranslocated E1 than of Endo H-treated, translocated E1 can be explained by retention of the signal sequence in the untranslocated protein. Consequently, we named this form of E1 "pre-E1." The nature of the two forms of E1 was confirmed by analyses of nonreduced samples (see below). Quantitations in three separate experiments showed that about 40 to 50% of E1 remained untranslocated.

An analysis under nonreducing conditions showed that fully oxidized E1 was produced in the SFV C-E1 RNA-transfected cells (see material that migrates like wild-type E1 in Fig. 2b, lanes 2, 4, 6, and 8). However, this E1 represented only a minor fraction of the translocated E1. This inefficiency in folding is evident from a comparison of the ratio of pre-E1 to fully oxidized E1 in the analyses of the nonreduced samples (Fig. 2b) and the ratio of pre-E1 to translocated E1 in the analyses of the reduced samples (Fig. 2a). It appears as if a large fraction of translocated E1, very soon after synthesis, enters a pool of disulfide-linked E1 aggregates. This material probably corresponds to the labelled material seen at the top of the separating gel and at the top of the concentrating gel in the analyses of the nonreduced samples (Fig. 2b, aggr). The nature of the aggregated material was further verified by immunoprecipitation analyses with an E1-specific antibody (see below).

To study the folding efficiency of E1 in more detail, a reduced, Endo H-treated sample and a nonreduced sample from transfected cells chased for 5 min were analyzed in the same gel (Fig. 2c). This analysis showed that translocated E1 had a higher mobility in the gel under nonreducing conditions. Furthermore, the amount of fully oxidized E1 (Fig. 2c, lane 3) was much lower than the amount of translocated (Endo H-sensitive) E1 seen in the reduced sample (lane 2). Quantitation of labelled E1 in three separate experiments showed that as much as 70 to 80% of the translocated E1 was engaged in disulfide-linked aggregates in cells transfected with SFV C-E1 RNA. In contrast, the pre-E1 band did not differ in mobility or in intensity in these analyses. Thus, it behaved like a typical cytoplasmic protein.

Synthesis of p62 in SFV C-p62 RNA-transfected cells. p62 chains from pulse-labelled cells were analyzed by SDS-PAGE under reducing conditions. This analysis showed two bands migrating in the region of control p62 (Fig. 3a, lanes 2, 4, 6, and 8). Endo H treatment of the samples demonstrated that the slower-migrating major band was sensitive to the enzyme, whereas the faster-migrating minor band was resistant (Fig. 3a, lanes 3, 5, 7, and 9). This result suggests that the slower-moving form represented glycosylated and hence translocated p62. The material in the faster-moving band was most likely p62 chains that were not translocated. Quantitations showed that this untranslocated fraction represented about 30% of the translated p62. We noted that the mobility of the glycosylated

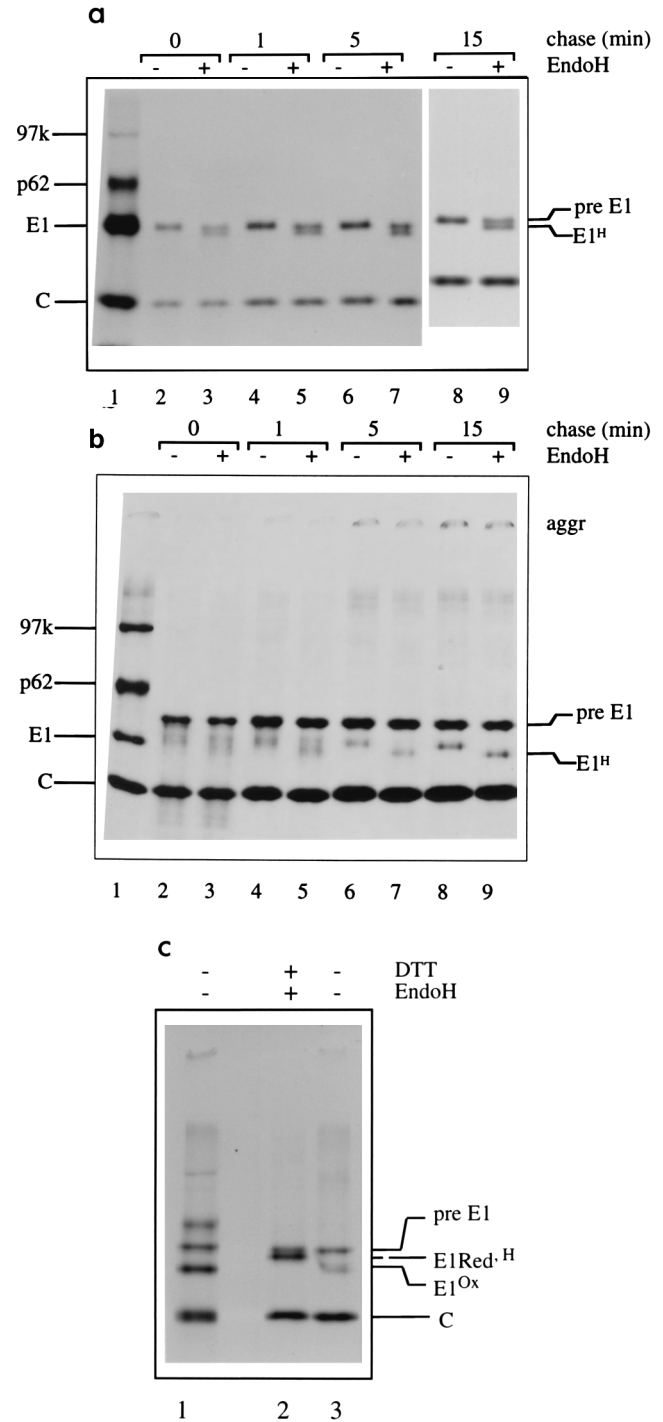


FIG. 2. Translocation and folding of E1 in cells transfected with SFV C-E1 RNA. Transfected cells were analyzed as described in the legend to Fig. 1. (a and b) Analyses of lysate samples under reducing (a) and nonreducing (b) conditions. (c) Equal portions of a reduced, Endo H-digested sample and a nonreduced sample from cells chased for 5 min were run next to each other. Lane 1 in all panels represents analyses of a control lysate from pulse-labelled cells transfected with SFV wild-type RNA. In panels a and b, analysis of the control shows bands corresponding to C, E1, p62, and 97-kDa proteins. In panel c, in which samples of chased cells were analyzed, the E2 protein (third band from the bottom) is shown as well. aggr, aggregates. Note that lanes 2 to 7 and lanes 8 and 9 in panel a were derived from different gels. Note also that the autoradiograph in panel b was exposed longer than that in panel a. See the legend to Fig. 1 for more details.

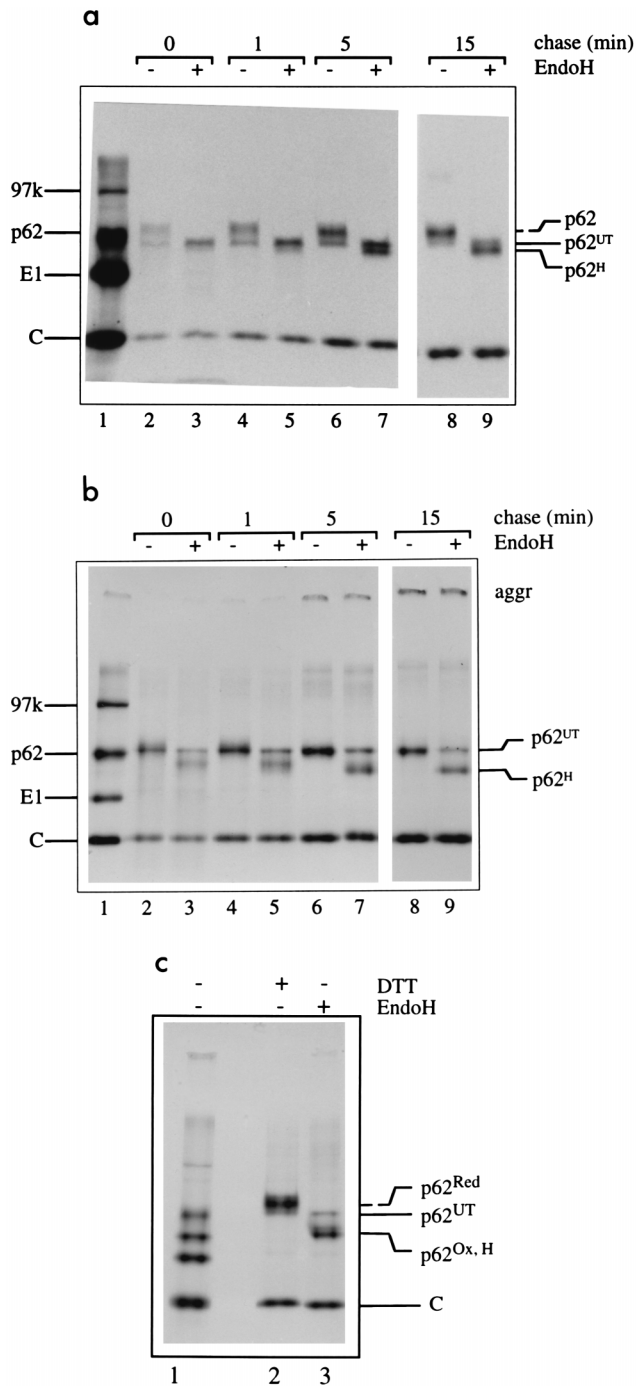


FIG. 3. Translocation and folding of p62 in cells transfected with SFV C-p62 RNA. Transfected cells were analyzed as described in the legend to Fig. 1. (a and b) Analyses of lysate samples under reducing (a) and nonreducing (b) conditions. (c) Equal portions of a reduced sample and a nonreduced, Endo H-digested sample from cells chased for 5 min were run next to each other. Lane 1 in all panels contains controls (see the legend to Fig. 2). Superscript UT, untranslocated; aggr, aggregates. Note that lanes 1 to 7 and lanes 8 and 9 in panels a and b were derived from different gels. See the legend to Fig. 1 for more details.

p62 band increased upon chase. Consequently, the Endo H-digested form, which comigrated with untranslocated p62 in samples chased for 0 or 1 min (Fig. 3a, lanes 3 and 5), migrated faster than untranslocated p62 in samples chased for 5 or 15

min (Fig. 3a, lanes 7 and 9). The reason for this change in the migration behavior of translocated p62 is not clear but might be related to processing at the p62-6K junction.

An analysis under nonreducing conditions showed that most of p62 appeared as a fully oxidized product already directly after the short pulse (Fig. 3b, lanes 2, 4, 6, and 8). This form comigrated with untranslocated p62 but could be separated after Endo H treatment (Fig. 3b, lanes 3, 5, 7, and 9). To quantitate the folding efficiency of p62, a reduced sample and a nonreduced, Endo H-treated sample, both from cells chased for 5 min, were run in parallel (Fig. 3c). This analysis showed that about 70% of translocated p62 was folded and oxidized correctly.

Synthesis of E1 and p62 in cells cotransfected with SFV C-p62 and SFV C-E1 RNAs. Our results obtained so far suggest that separate expression of the E1 protein results in reduced translocation of E1 chains across the ER membrane and further in a significant misfolding of the translocated E1 chains. They also suggest that the p62 protein facilitates E1 maturation when both proteins are expressed from the same coding unit on the 26S RNA. In order to find out whether this effect of p62 could also be mediated in *trans*, that is, by p62 synthesized from a separate coding unit, we performed a co-expression experiment with SFV C-p62 and SFV C-E1 RNAs. We wanted to express p62 with an excess of E1 in the same cells. To meet these conditions, we used 10 and 30 μ l of SFV C-E1 and SFV C-p62 RNAs, respectively, for transfection. The cotransfected cells were pulse-labelled as described above and chased for either 5 or 15 min. The p62 and E1 expression frequencies were monitored in parallel cultures by immunofluorescence analyses of viral proteins. Coexpression was seen in 70 to 80% of the cells. Reduced, Endo H-treated samples and nonreduced samples were prepared from the pulse-labelled cultures and analyzed by SDS-PAGE. Quantitation of p62 and E1 bands showed that the corresponding proteins were translated in an approximately 3:1 ratio. The ratio of translocated p62 and E1 was approximately 4:1. However, despite the excess of p62, E1 translocation and folding into a correct structure were only slightly improved. Quantitation from three separate experiments showed that about 60% of E1 was translocated and that about 40% of E1 was folded correctly under these conditions. Figure 4 shows the results of one such analysis with a lysate of cells chased for 5 min. An analysis of a reduced, Endo H-treated sample (Fig. 4, lane 2) showed the p62 and E1 proteins as upper and lower band doublets, respectively. The upper, p62 doublet consisted of a weaker band with a lower mobility, representing untranslocated p62, and a stronger band with a higher mobility, representing translocated p62. The lower, E1 doublet consisted of the slower-moving pre-E1 and the faster-moving translocated E1. In the corresponding analysis of the nonreduced sample (Fig. 4, lane 3), the translocated and untranslocated p62 proteins migrated as one thick band, whereas the pre-E1 and oxidized E1 proteins were clearly separated into slower- and faster-moving bands, respectively. Note the difference in the band intensities of reduced, Endo H-digested E1 in lane 2 and oxidized E1 in lane 3.

To find out whether oxidized E1 could form heterodimers with coexpressed p62, we used a previously described immunoprecipitation assay (70). In this assay, an anti-E1 monoclonal antibody, UM 8.139, is used to precipitate p62-E1 complexes from a lysate of transfected or infected cells. We first analyzed the reactivity of this antibody to E1 that had been expressed in cells transfected with only SFV C-E1 RNA. The antibody was shown to react both with correctly oxidized E1 and with the disulfide-linked protein aggregates but not with pre-E1 (data not shown). These results confirmed the E1 nature of the

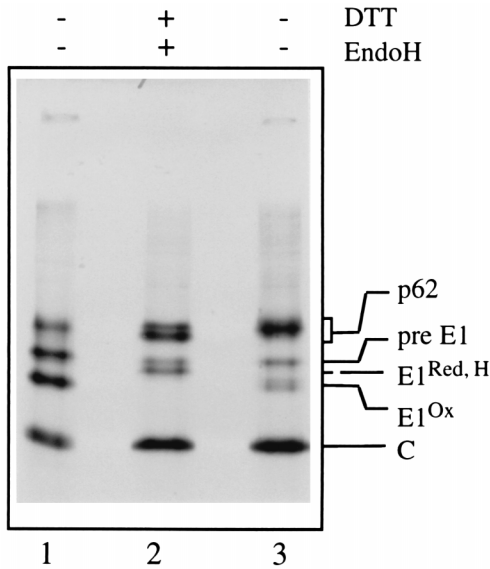


FIG. 4. Translocation and folding of viral membrane proteins in cells cotransfected with SFV C-E1 and SFV C-p62 RNAs. Cells were transfected with both SFV C-E1 and SFV C-p62 RNAs at a 1:3 ratio. They were then labelled as described in the legend to Fig. 1 and chased for 5 min. A lysate was prepared, and samples were either reduced and Endo H treated or mock treated. Equal amounts of each sample were analyzed by SDS-PAGE. Lane 1 shows analysis of a control lysate.

aggregates. Apparently the antibody recognized all translocated forms of E1, both correctly and incorrectly oxidized ones. For the heterodimer assay, cells were cotransfected (with excess SFV C-p62 RNA), pulse-labelled for 15 min, and chased for 5, 30, and 60 min. Analyses of the immunoprecipitates from lysates of cells chased for 5 min clearly showed the presence of both p62 and E1 (Fig. 5, lanes 1 and 2). This result suggests that heterodimers were formed in *trans* between translocated E1 and p62. Most likely this process involved the correctly

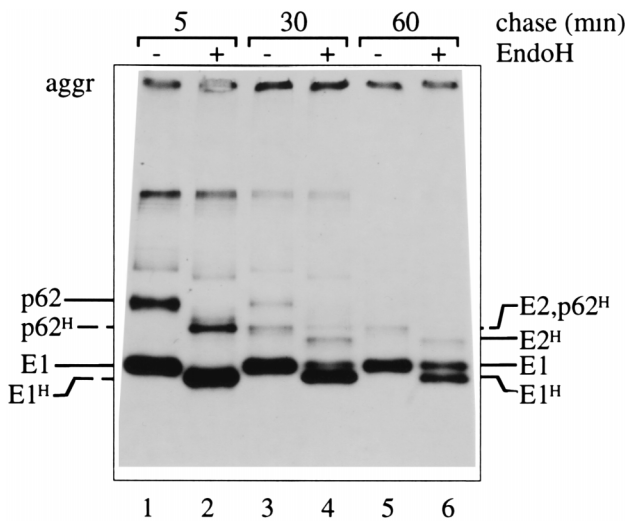


FIG. 5. Heterodimerization in *trans*. Cells were cotransfected with SFV C-E1 and SFV C-p62 RNAs, labelled for 15 min, and chased for 5, 30, or 60 min. Cell lysates were precipitated with a monoclonal antibody which reacted with translocated E1 protein but not with untranslocated pre-E1 protein and were either mock treated (lanes 1, 3, and 5) or Endo H treated (lanes 2, 4, and 6). Samples were analyzed by SDS-PAGE under nonreducing conditions. aggr, aggregates.

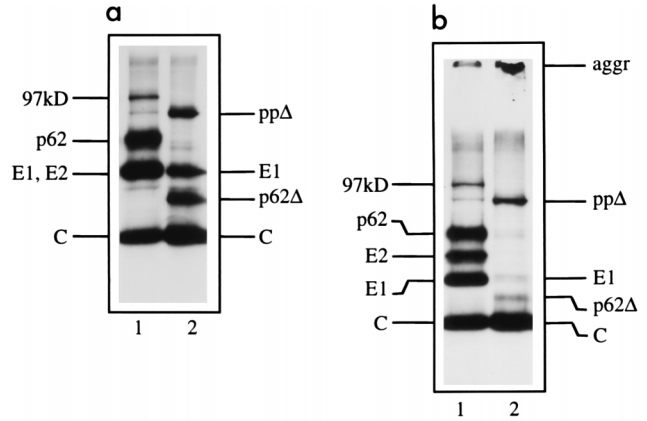


FIG. 6. Translocation and folding of viral membrane proteins in SFV p62Δc RNA-transfected cells. Cells transfected with SFV p62Δc RNA were labelled for 15 min and chased for 30 min. The lysate was analyzed under reducing (a, lane 2) and nonreducing (b, lane 2) conditions by SDS-PAGE. ppΔ, uncleaved and untranslocated p62Δc-6K-E1 polyprotein; p62Δ, translocated p62 fragment; aggr, aggregates. Lane 1 in both panels shows analyses of control lysates.

oxidized fractions of these membrane proteins. Analyses of the chased samples showed that coprecipitated p62 was cleaved into E2, which was partially Endo H resistant (Fig. 5, lanes 3 to 6), and further that about half of the E1 molecules were processed into a completely Endo H-resistant form (Fig. 5, lane 6). These modifications imply that wild-type-like heterodimers assembled in the ER and also that they were transported along the exocytotic pathway beyond the trans-Golgi apparatus, most likely all the way to the cell surface (3a, 20, 47, 65). Note that all exported heterodimers were subject to significant degradation during the chase. Also note the aggregated material, which probably represented mostly E1. We conclude that a significant fraction (about 50%) of correctly folded E1 can form heterodimers with p62 expressed from a separate coding unit.

Analysis of E1 translocation and folding in cells transfected with SFV RNA mutants with deletions in the p62 gene region. The results described above suggest that p62 can only support E1 translocation and folding efficiently if it originates from the same translation unit as E1. A further question was whether the E1 maturation-facilitating function of p62 was mediated by a subdomain of p62 or by the whole molecule. To address this question, we made several internal deletions in the p62 gene of the viral genome (see description of pSFV-p62Δ constructs in Materials and Methods) and analyzed membrane protein synthesis after RNA transfection described above. We found that for all mutants, about 60 to 70% of the p62Δ and E1 chains were inserted into the ER membrane according to the expected topology. However, most (about 80%) of the inserted chains were engaged in disulfide-linked aggregates. This result is exemplified in Fig. 6 by the analyses of viral proteins from cells transfected with SFV p62Δc RNA. Analyses of the reduced samples showed untranslocated p62Δ-6K-E1 polyprotein (ppΔ) and translocated E1 and p62Δ (Fig. 6a, lane 2). The glycosylated nature of the latter two proteins was demonstrated by Endo H digestion (data not shown). Analyses of the corresponding nonreduced samples showed very little correctly oxidized E1 protein and the p62 fragment (Fig. 6b, lane 2). Most of these proteins appeared to be aggregated at the top of the separating gel. Thus, we were unable to assign the E1 maturation-facilitating function of p62 to a specific subdomain of the p62 protein.

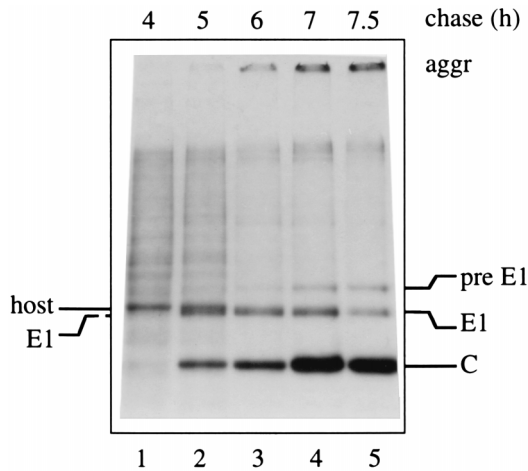


FIG. 7. Translocation and folding of E1 at early times after transfection of cells with SFV C-E1 RNA. Cell cultures were radiolabelled for 15 min and chased for 30 min at different times after transfection with SFV C-E1 RNA. The cells were then lysed, and the lysates were analyzed by SDS-PAGE under non-reducing conditions followed by fluorography. The times indicated correspond to the times at which the pulses were initiated. Note that many host proteins are synthesized at early times after transfection. One of these, designated "host," migrates just above the E1 protein in lanes 1 and 2. aggr, aggregates.

E1 folding at a lower level of E1 expression. In all of the experiments described above, the viral proteins were expressed at levels corresponding to those of a wild-type SFV infection. This level is very high. Measurements of viral protein synthesis at 7 h postinfection, which corresponds approximately to the time for our present experiments, showed that this synthesis equals one-third of the total protein synthesis in uninfected cells (30). Host protein synthesis is already inhibited 4 to 5 h postinfection. Under these conditions, limiting amounts of folding-facilitating factors might be available to the viral membrane proteins in the ER. The E1 protein could be especially sensitive to this condition and therefore forms disulfide-linked aggregates. This possibility was investigated by analyzing the folding efficiency of E1 when it was produced at reduced levels. The lower levels of E1 synthesis were obtained in two ways: (i) by studying E1 synthesis in SFV C-E1 RNA-transfected cells at times after transfection earlier than those used before in this study and (ii) by using the low-level-expression vector pSFV-E1 instead of the high-level-expression vector pSFV-C-E1. According to the first approach, we pulse-labelled (15 min) and chased (30 min) SFV C-E1 RNA-transfected cells at 4, 5, 6, 7, and 7.5 h posttransfection and analyzed the viral proteins by SDS-PAGE under nonreducing conditions. The results are shown in Fig. 7. At 4 h posttransfection, no viral proteins could yet be detected. Host proteins were still being produced; most notably, there was a strong, host-derived protein band migrating at a position just above that of E1 (labelled "host" in Fig. 7, lane 1). At 5 h posttransfection, the C protein started to become synthesized. In addition, E1 was appearing. This was seen as a downward widening of the still-visible host protein band. At 6 h posttransfection, the synthesis of the host protein was clearly inhibited and the expression of E1 became more pronounced. Most importantly, the pre-E1 and disulfide-linked E1 aggregates did not appear until 7 h posttransfection. This result showed that E1 translocation and folding were impeded with time after transfection, when the level of E1 synthesis increased. This finding was confirmed by expression of E1 from SFV E1 RNA. This RNA lacks the C protein-encoding region, which acts as a powerful potentiator of polyprotein translation

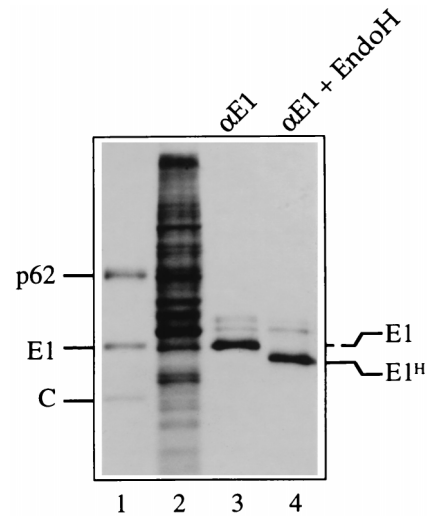


FIG. 8. Translocation and folding of the E1 protein in cells transfected with SFV E1 RNA. Transfected cells were labelled for 15 min and chased for 30 min. Cell lysates were analyzed by SDS-PAGE under nonreducing conditions. Lanes: 1, control lysate; 2, analysis of a lysate from SFV E1 RNA-transfected cells; 3 and 4, immunoprecipitates, either mock treated (lane 3) or Endo H treated (lane 4), of the same lysate obtained with a polyclonal antibody directed against the E1 protein. Note the absence of pre-E1 and E1 aggregates.

from the viral subgenome (62). Therefore, E1 protein production in SFV E1 RNA-transfected cells was reduced to about 1/10 to 1/20 that in SFV C-E1 RNA-transfected cells. Figure 8 shows SDS gel analyses under nonreducing conditions of pulse-labelled E1 protein from SFV E1 RNA-transfected cells. The chase was for 15 min. In this case, E1 was immunoprecipitated with a polyclonal anti-E1 antibody that reacted with all forms of E1. The results showed that almost only correctly oxidized E1 was produced. Two less intense, slower-migrating bands were also seen. The migration of the slower one corresponded to that of pre-E1. However, as this band appeared to be Endo H sensitive, it could not represent pre-E1 but more likely was a host protein contaminant.

DISCUSSION

In this study, we showed that the large majority of the E1 and p62 proteins expressed from the wild-type common coding unit and inserted into the ER membrane oxidize and fold correctly. From earlier studies, we know that they also heterodimerize very efficiently (4). However, when E1 was expressed separately, we found that most of the inserted E1 (70 to 80%) malformed into disulfide-linked aggregates. In contrast, the separate expression of p62 resulted in the correct oxidation and folding of the bulk of the inserted chains (70%). This result suggests that the correct folding of E1 but not of p62 is dependent on the formation of an E1-p62 heterodimer. This dependence was shown to be conditional in that low expression of E1 resulted in the correct folding of virtually all of the inserted E1 chains.

Recently, Carleton et al. reported on a study of Sindbis virus (SIN) E1 synthesis (16). Their major conclusion was completely opposite to ours, that is, that E1 can fold correctly, independently of PE2 (PE2 corresponds to p62 in SFV) and heterodimerization. However, in that study, the possible formation of malformed E1 was not investigated. The analyses focused only on the fraction of E1 which was able to fold correctly. Furthermore, according to their pulse-labelling pro-

together, they studied E1 synthesis at a time which represented 5 h after the start of infection. We show here that, at a corresponding time after SFV C-E1 RNA transfection, viral protein synthesis was still far from its maximum in cells (Fig. 7). At this early time, we were also unable to detect heterodimerization-dependent folding of E1. Therefore, we conclude that under conditions of high-level expression of the viral membrane proteins, as occurs during a fulminant infection of cells, E1 folding is highly dependent on E1 oligomerization with p62. This means that p62 acts normally as a chaperone for E1. If no p62 is available, the cells can apparently provide chaperones, but only to a certain limit, which corresponds to 20 to 30% of the inserted E1. The apparently correctly oxidized fraction of E1 formed under these circumstances was found to be competent for oligomerization *in trans* with p62 expressed from a separate coding unit.

With pulse-chase analyses, we demonstrated that the mal-folding of E1 occurred very rapidly after E1 synthesis. Most of the translocated E1 was already found to be engaged in disulfide-linked aggregates 5 min after a 2-min pulse. This result suggests that the E1-p62 heterodimerization reaction, which prevents extensive E1 aggregation in SFV wild-type RNA-transfected cells, must be a very early event. Furthermore, our present results, which showed that separately expressed p62 cannot significantly prevent E1 mal-folding, and our earlier results, which showed that such p62 cannot compete for E1 expressed from a wild-type-linked common coding unit, suggest that there is a coupling between the efficient folding and heterodimerization of E1 on the one hand and the expression of both membrane proteins from a common coding unit on the other. As an explanation, we suggest a translocon-facilitated heterodimerization model for p62 and E1. According to this model, p62 does not leave the ER translocon after it has been translated and translocated but stays inside and waits until the subsequently translated E1 has also been translocated. This strategy allows the two chains the chance to heterodimerize while still localized at their common site of synthesis.

Our model for p62-E1 complex formation has interesting similarities with the one recently proposed for the biogenesis of polytopic membrane proteins (9; see also reference 21). According to the latter, membrane segments of a multispanning membrane protein assemble within the translocon before they integrate into the lipid bilayer. The translocon is closed laterally during the entire round of translation of the polytopic protein so that the first membrane segment cannot be released into the lipid membrane but has to await inside until all trans-membrane segments have been synthesized. If one disregards the cotranslational cleavage events of the SFV polyprotein, it resembles a polytopic membrane protein.

It is conceivable that p62 forms complexes with a folding intermediate of E1. This possibility was recently supported by data obtained with SIN. During the biogenesis of SIN E1, three folding intermediates were identified (49). With a *ts* mutant of SIN (*ts23*) at the permissive temperature of 28°C, it was possible to slow down the kinetics of E1 folding and heterodimerization so much that E1 folding and heterodimerization could be correlated with each other (15). Coimmunoprecipitation analyses with an E1 antibody showed that the second and third E1 folding intermediates became complexed with PE2. The results suggest that SIN E1 becomes complexed with PE2 before its folding is completed.

It is noteworthy that our heterodimerization model can give a satisfactory explanation of how it is possible to synthesize E1 with an inducible fusion function. According to this model, p62, through complex formation with newly made E1, helps the latter to fold into a certain metastable conformation with a

latent fusion function. p62 then continues to chaperone this form of E1 through the whole stage of virus assembly in the form of the p62-E1 complex and also, thereafter, in the virus particle, in the form of the E2-E1 complex. Inside the endosome of an uninfected cell, where the low pH will dissociate E1 from E2, the p62-E2 chaperoning of E1 is brought to an end. Consequently, E1 forms a homotrimer, and its fusion function is activated. It follows from this discussion that the E1 folding and E1-p62 oligomerization mechanisms represent the first parts of the overall mechanism by which SFV controls its fusion activity.

In this work, we also analyzed the translocation efficiencies of p62 and E1. These were found to be significantly impaired even when the two proteins were expressed from a common coding unit. As much as 30% of the p62 and E1 protein chains remained untranslocated. This inefficiency in chain translocation might have been due to the selective overproduction of the p62 and E1 membrane proteins and the simultaneous shut-off of host protein synthesis in the transfected cells. The lowest translocation efficiency was found for the separately expressed E1. In this case, only half of the chains were successfully translocated. It is possible that the formation of the abundant disulfide-linked E1 aggregates impaired the translocation function of the ER membrane. This effect might have been mediated by ER folding factors, because at least in yeast these have been shown to interact with the translocation machinery and to play a role in the translocation process (43, 60). Not surprisingly, the translocation efficiency of separately expressed E1 was much better in experiments where E1 was produced at lower levels.

ACKNOWLEDGMENTS

We thank Leena Rinnevu for cell cultures and Ingrid Sigurdson for typing. We are also grateful to Dirk-Jan Opstelten and Mathilda Sjöberg for critical reading of the manuscript.

This work was supported by EU grants CHRX-CT94-0496 and CHRX-CT92-0018 and Swedish Natural Science Research Council grant B-AA-/BU 09353-311.

REFERENCES

1. Aliperti, G., and M. J. Schlesinger. 1978. Evidence for an autoprotease activity of Sindbis virus capsid protein. *Virology* **90**:366-369.
2. Allison, S. L., J. Schlich, K. Stiasny, C. W. Mandl, C. Kunz, and K. X. Heinz. 1995. Oligomeric rearrangement of tick-borne encephalitis virus envelope proteins induced by an acidic pH. *J. Virol.* **69**:695-700.
3. Baron, M. D., and K. Forsell. 1991. Oligomerization of the structural proteins of Rubella virus. *Virology* **185**:811-819.
- 3a. Barth, B.-U., and H. Garoff. Unpublished data.
4. Barth, B.-U., J. M. Wahlberg, and H. Garoff. 1995. The oligomerization reaction of the Semliki Forest virus membrane protein subunits. *J. Cell Biol.* **128**:283-291.
5. Blacklow, S. C., M. Lu, and P. S. Kim. 1995. A trimeric subdomain of the simian immunodeficiency virus envelope glycoprotein. *Biochemistry* **34**:14955-14962.
6. Boege, U., G. Wengler, G. Wengler, and B. Wittman-Liebold. 1981. Primary structure of the core proteins of the alphaviruses Semliki Forest virus and Sindbis virus. *Virology* **113**:293-303.
7. Boere, W. A. M., T. Harmsen, J. Vinje, B. J. Benaissa-Trouw, C. A. Kraaijeveld, and H. Snippe. 1984. Identification of distinct antigenic determinants on Semliki Forest virus by using monoclonal antibodies with different antiviral activities. *J. Virol.* **52**:575-582.
8. Bonatti, S., and G. Blobel. 1979. Absence of a cleavable signal sequence in Sindbis virus glycoprotein PE2. *J. Biol. Chem.* **254**:12261-12264.
9. Borel, A. C., and S. M. Simon. 1996. Biogenesis of polytopic membrane proteins: membrane segments assemble within translocation channels prior to membrane integration. *Cell* **85**:379-389.
10. Boulay, F., R. W. Doms, R. G. Webster, and A. Helenius. 1988. Posttranslational oligomerization and cooperative acid activation of mixed influenza hemagglutinin trimers. *J. Cell Biol.* **106**:629-639.
11. Braakman, I., H. Hoover-Litty, K. R. Wagner, and A. Helenius. 1991. Folding of influenza hemagglutinin in the endoplasmic reticulum. *J. Cell Biol.* **114**:401-411.

12. **Bron, R., J. M. Wahlberg, H. Garoff, and J. Wilschut.** 1993. Membrane fusion of Semliki Forest virus in a model system: correlation between fusion kinetics and structural changes in the envelope glycoprotein. *EMBO J.* **12**:693–701.
13. **Brown, D. T., and J. F. Smith.** 1975. Morphology of BHK-21 cells infected with Sindbis virus temperature-sensitive mutants in complementation groups D and E. *J. Virol.* **15**:1262–1266.
14. **Bullough, P. A., F. M. Hugson, J. J. Skehel, and D. C. Wiley.** 1994. Structure of influenza haemagglutinin at the pH of membrane fusion. *Nature* **371**:37–43.
15. **Carleton, M., and D. T. Brown.** 1996. Events in the endoplasmic reticulum abrogate the temperature sensitivity of Sindbis virus mutant *ts23*. *J. Virol.* **70**:952–959.
16. **Carleton, M., H. Lee, M. Mulvey, and D. T. Brown.** 1997. Role of glycoprotein PE2 in formation and maturation of the Sindbis virus spike. *J. Virol.* **71**:1558–1566.
17. **Carr, C. M., and P. S. Kim.** 1993. A spring-loaded mechanism for the conformational change in influenza hemagglutinin. *Cell* **73**:823–832.
18. **Cheng, H. R., R. J. Kuhn, N. H. Olson, M. G. Rossmann, H.-K. Choi, T. J. Smith, and T. S. Baker.** 1995. Nucleocapsid and glycoprotein organization in an enveloped virus. *Cell* **80**:621–630.
19. **Choi, H.-K., L. Tong, W. Minor, P. Dumas, U. Boege, M. G. Rossmann, and G. Wengler.** 1991. Structure of Sindbis virus core protein reveals a chymotrypsin-like serine proteinase and the organization of the virion. *Nature* **354**:37–43.
20. **de Curtis, I., and K. Simons.** 1988. Dissection of Semliki Forest virus glycoprotein delivery from the trans-Golgi network to the cell surface in permeabilized BHK cells. *Proc. Natl. Acad. Sci. USA* **85**:8052–8056.
21. **Do, H., D. Falcone, J. Lin, D. W. Andrews, and A. E. Johnson.** 1996. The cotranslational integration of membrane proteins into the phospholipid bilayer is a multistep process. *Cell* **85**:369–378.
22. **Doms, R. W., and A. Helenius.** 1986. Quaternary structure of influenza virus hemagglutinin after acid treatment. *J. Virol.* **60**:833–839.
23. **Fass, D., S. C. Harrison, and P. S. Kim.** 1996. Retrovirus envelope domain at 1.7 Å resolution. *Nature Struct. Biol.* **3**:465–469.
24. **Fass, D., and P. S. Kim.** 1995. Dissection of a retrovirus envelope protein reveals structural similarity to influenza hemagglutinin. *Curr. Biol.* **5**:1377–1383.
25. **Fuller, S. D., J. A. Berriman, S. J. Butcher, and B. E. Gowen.** 1995. Low pH induces swiveling of the glycoprotein heterodimers in the Semliki Forest virus spike complex. *Cell* **81**:715–725.
26. **Garoff, H., A.-M. Frischauf, K. Simons, H. Lehrach, and H. Delius.** 1980. Nucleotide sequence of cDNA coding for Semliki Forest virus membrane glycoproteins. *Nature* **288**:236–241.
27. **Garoff, H., D. Huylebroeck, A. Robinson, U. Tillman, and P. Liljeström.** 1990. The signal sequence of the p62 protein of Semliki Forest virus is involved in initiation but not in completing chain translocation. *J. Cell Biol.* **111**:867–876.
28. **Garoff, H., C. Kondor-Koch, and H. Riedel.** 1982. Structure and assembly of alphaviruses. *Curr. Top. Microbiol. Immunol.* **99**:1–50.
29. **Garoff, H., K. Simons, and B. Dobberstein.** 1978. Assembly of Semliki Forest virus membrane glycoproteins in the membrane of the endoplasmic reticulum in vitro. *J. Mol. Biol.* **124**:587–600.
30. **Garry, R. F.** 1994. Sindbis virus-induced inhibition of protein synthesis is partially reversed by medium containing an elevated potassium concentration. *J. Gen. Virol.* **75**:411–415.
31. **Hahn, C. S., and J. H. Strauss.** 1990. Site-directed mutagenesis of the proposed catalytic amino acids of the Sindbis virus capsid protein autoprotease. *J. Virol.* **64**:3069–3073.
32. **Hashimoto, K., S. Erdei, S. Keränen, J. Saraste, and L. Käriäinen.** 1981. Evidence for a separate signal sequence for the carboxy-terminal envelope glycoprotein E1 of Semliki Forest virus. *J. Virol.* **38**:34–40.
33. **Heinz, F. X., K. Stiasny, G. Püschner-Auer, H. Holzmann, S. L. Allison, C. W. Mandl, and C. Kunz.** 1994. Structural changes and functional control of the tick-borne encephalitis virus glycoprotein E by the heterodimeric association with protein prM. *Virology* **198**:109–117.
34. **Horton, R., H. Hunt, S. Ho, J. Pullen, and L. Pease.** 1989. Engineering hybrid genes without the use of restriction enzymes: gene splicing by overlap extension. *Gene* **77**:61–68.
35. **Hunter, E.** 1994. Macromolecular interactions in the assembly of HIV and other retroviruses. *Virology* **5**:71–83.
36. **Justman, J., M. R. Klimjack, and M. Kielian.** 1993. Role of spike protein conformational changes in fusion of Semliki Forest virus. *J. Virol.* **67**:7579–7607.
37. **Kielian, M., M. R. Klimjack, S. Ghosh, and W. A. Duffus.** 1996. Mechanisms of mutations inhibiting fusion and infection by Semliki Forest virus. *J. Cell Biol.* **134**:863–872.
38. **Klenk, H.-D., and R. Rott.** 1988. The molecular biology of influenza virus pathogenicity. *Adv. Virus Res.* **34**:247–281.
39. **Liljeström, P., and H. Garoff.** 1991. Internally located cleavable signal sequences direct the formation of Semliki Forest virus membrane proteins from a polyprotein precursor. *J. Virol.* **65**:147–154.
40. **Liljeström, P., S. Lusa, D. Huylebroeck, and H. Garoff.** 1991. In vitro mutagenesis of a full-length cDNA clone of Semliki Forest virus: the 6,000-molecular-weight membrane protein modulates virus release. *J. Virol.* **65**:4107–4113.
41. **Lobigs, M., and H. Garoff.** 1990. Fusion function of the Semliki Forest virus spike is activated by proteolytic cleavage of the envelope glycoprotein p62. *J. Virol.* **64**:1233–1240.
42. **Lu, M., S. C. Blacklow, and P. S. Kim.** 1995. A trimeric structural domain of the HIV-1 transmembrane glycoprotein. *Nature Struct. Biol.* **2**:1075–1082.
43. **Lyman, S. K., and R. Schekman.** 1995. Interaction between BiP and Sec63p is required for the completion of protein translocation into the ER of *Saccharomyces cerevisiae*. *J. Cell Biol.* **131**:1163–1171.
44. **Marsh, M., E. Bolzau, and A. Helenius.** 1983. Penetration of Semliki Forest virus from acidic prelysosomal vacuoles. *Cell* **32**:931–940.
45. **Matlin, K. S., H. Reggio, A. Helenius, and K. Simons.** 1981. Infectious entry pathway of influenza virus in a canine kidney cell line. *J. Cell Biol.* **91**:601–613.
46. **Melancon, P., and H. Garoff.** 1987. Processing of the Semliki Forest virus structural polyprotein: role of the capsid protease. *J. Virol.* **61**:1301–1309.
47. **Melancon, P., and H. Garoff.** 1986. Reinitiation of translocation in the Semliki Forest virus structural polyprotein: identification of the signal for the E1 glycoprotein. *EMBO J.* **5**:1551–1560.
48. **Mulvey, M., and D. T. Brown.** 1996. Assembly of the Sindbis virus spike protein complex. *Virology* **219**:125–132.
49. **Mulvey, M., and D. T. Brown.** 1994. Formation and rearrangement of disulfide bonds during maturation of the Sindbis virus E1 glycoprotein. *J. Virol.* **68**:805–812.
50. **Mulvey, M., and D. T. Brown.** 1995. Involvement of the molecular chaperone BiP in maturation of Sindbis virus envelope glycoprotein. *J. Virol.* **69**:1621–1627.
51. **Omar, A., and H. Koblet.** 1988. Semliki Forest virus particles containing only the E1 envelope glycoprotein are infectious and can induce cell-cell fusion. *Virology* **166**:17–23.
52. **Paredes, A. M., D. T. Brown, R. Rothnagel, W. Chiu, R. J. Schoepp, R. E. Johnston, and B. V. V. Prasad.** 1993. Three-dimensional structure of a membrane-containing virus. *Proc. Natl. Acad. Sci. USA* **90**:9095–9099.
53. **Patterson, S., J. Gross, and J. S. Oxford.** 1988. The intracellular distribution of influenza virus matrix protein and nucleoprotein in infected cells and their relationship to haemagglutinin in the plasma membrane. *J. Gen. Virol.* **69**:1859–1872.
54. **Ralston, R., K. Thudium, K. Berger, C. Kuo, B. Gervase, J. Hall, M. Selby, G. Kuo, M. Houghton, and Q.-L. Choo.** 1993. Characterization of hepatitis C virus envelope glycoprotein complexes expressed by recombinant vaccinia viruses. *J. Virol.* **67**:6753–6761.
55. **Rice, C. M., and J. H. Strauss.** 1982. Association of Sindbis virion glycoproteins and their precursors. *J. Mol. Biol.* **154**:325–348.
56. **Rice, C. M., and J. H. Strauss.** 1981. Nucleotide sequence of the 26S mRNA of Sindbis virus and deduced sequence of the encoded virus structural proteins. *Proc. Natl. Acad. Sci. USA* **78**:2062–2066.
57. **Ruigrok, R. W. H., A. Aitken, L. J. Calder, S. R. Martin, J. J. Skehel, S. A. Wharton, W. Weis, and D. C. Wiley.** 1988. Studies on the structure of the influenza virus haemagglutinin at the pH of membrane fusion. *J. Gen. Virol.* **69**:2785–2795.
58. **Rümenapf, T., G. Unger, J. H. Strauss, and H.-J. Thiel.** 1993. Processing of the envelope glycoproteins of pestiviruses. *J. Virol.* **67**:3288–3294.
59. **Salminen, A., J. M. Wahlberg, M. Lobigs, P. Liljeström, and H. Garoff.** 1992. Membrane fusion process of Semliki Forest virus. II. Cleavage dependent reorganization of the spike protein complex controls virus entry. *J. Cell Biol.* **116**:349–357.
60. **Sanders, S. L., K. M. Whitfield, J. P. Vogel, M. D. Rose, and R. W. Schekman.** 1992. Sec61p and BiP directly facilitate polypeptide translocation into the ER. *Cell* **69**:353–365.
61. **Sekikawa, K., and C.-J. Lai.** 1983. Defects in functional expression of an influenza virus hemagglutinin lacking the signal peptide sequences. *Proc. Natl. Acad. Sci. USA* **80**:3563–3567.
62. **Sjöberg, M., M. Suomalainen, and H. Garoff.** 1994. A significantly improved Semliki Forest virus expression system based on translation enhancer segments from the viral capsid gene. *Bio/Technology* **12**:1127–1131.
63. **Smyth, J., M. Suomalainen, and H. Garoff.** 1997. Efficient multiplication of a Semliki Forest virus chimera containing Sindbis virus spikes. *J. Virol.* **71**:818–823.
64. **Stieneke-Gröber, A., M. Vey, H. Angliker, E. Shaw, G. Thomas, C. Roberts, H.-D. Klenk, and W. Garten.** 1992. Influenza virus hemagglutinin with multi-basic cleavage site is activated by furin, a subtilisin-like endoprotease. *EMBO J.* **7**:2407–2414.
65. **Suomalainen, M., and H. Garoff.** 1994. Incorporation of homologous and heterologous proteins into the envelope of Moloney murine leukemia virus. *J. Virol.* **68**:4879–4889.
66. **Suomalainen, M., P. Liljeström, and H. Garoff.** 1992. Spike protein-nucleocapsid interactions drive the budding of alphaviruses. *J. Virol.* **66**:4737–4747.
67. **Tatu, U., C. Hammond, and A. Helenius.** 1995. Folding and oligomerization

- of influenza hemagglutinin in the ER and the intermediate compartment. *EMBO J.* **14**:1340–1348.
68. **Vogel, R. H., S. W. Provencher, C.-H. von Bonsdorff, M. Adrian, and J. Dubochet.** 1986. Envelope structure of Semliki Forest virus reconstructed from cryo-electron micrographs. *Nature* **320**:533–535.
69. **Wahlberg, J., and H. Garoff.** 1992. Membrane fusion process of Semliki Forest virus. I. Low pH-induced rearrangement in spike protein quaternary structure precedes virus penetration into cells. *J. Cell Biol.* **116**:339–348.
70. **Wahlberg, J. M., W. A. Boere, and H. Garoff.** 1989. The heterodimeric association between the membrane proteins of Semliki Forest virus changes its sensitivity to mildly acidic pH during virus maturation. *J. Virol.* **63**:4991–4997.
71. **Wahlberg, J. M., R. Bron, J. Wilschut, and H. Garoff.** 1992. Membrane fusion of Semliki Forest virus involves homotrimers of the fusion protein. *J. Virol.* **66**:7309–7318.
72. **Wengler, G., and G. Wengler.** 1989. Cell-associated West Nile flavivirus is covered with E+Pre-M protein heterodimers which are destroyed and re-organized by proteolytic cleavage during virus release. *J. Virol.* **63**:2521–2526.
73. **White, J. M.** 1992. Membrane fusion. *Science* **258**:917–924.
74. **Wiley, D. C., and J. J. Skehel.** 1987. The structure and function of the hemagglutinin membrane glycoprotein of influenza virus. *Annu. Rev. Biochem.* **56**:365–394.
75. **Wilson, I., J. Skehel, and D. Wiley.** 1981. Structure of the haemagglutinin membrane glycoprotein in influenza virus at 3 Å resolution. *Nature (London)* **292**:366–373.
76. **Yon, J., and M. Fried.** 1989. Precise gene fusion by PCR. *Nucleic Acids Res.* **17**:4895.
77. **Ziemiacki, A., and H. Garoff.** 1978. Subunit composition of the membrane glycoprotein complex of Semliki Forest virus. *J. Mol. Biol.* **122**:259–269.
78. **Ziemiacki, A., H. Garoff, and K. Simons.** 1980. Formation of the Semliki Forest virus membrane glycoprotein complexes in the infected cell. *J. Gen. Virol.* **50**:111–123.